

# Real Time Control of an Induction Motor Using IMC Approach

Duong Hoai Nghia<sup>†</sup>, Nguyen Van Nho<sup>\*</sup>, Nguyen Xuan Bac<sup>\*</sup>, and Hong-Hee Lee<sup>\*\*</sup>

<sup>†\*</sup> Faculty of Electrical & Electronics Engineering, University of Technology, Ho Chi Minh, Vietnam

<sup>\*\*</sup> School of Electrical Engineering, University of Ulsan, Ulsan, Korea

## ABSTRACT

The paper presents a method for controlling induction motors using a nonlinear internal model control (IMC) approach. The process model and the inverse model are developed in the rotor flux coordinate. The main advantage of the proposed method is that it easily specifies the performance (steady state error, transient response, etc.) and the robustness of the controller by means of the IMC filters. Simulation results illustrate the effectiveness of the proposed method. Results on a real time system show that the control system has good performance and robustness against changes in motor parameters (rotor and stator resistances, rotor and stator inductances, rotor inertia).

**Keywords:** Nonlinear internal model control, Induction motor, Real time control, Three-level inverter

## 1. Introduction

The induction motor is widely used in industry because of its reliability and low cost. However, since the dynamic model of an induction motor is strongly nonlinear, the control of an induction motor is a challenging problem and has attracted much attention. Many methods have been proposed and can be mentioned as follows:

- Field-oriented control (FOC) <sup>[1], [2], [3]</sup>
- Direct torque control (DTC) <sup>[4], [5], [3]</sup>
- Passivity-based control <sup>[6], [7]</sup>
- Sliding mode control <sup>[8], [9]</sup>

- Input-output linearization by state feedback <sup>[10]</sup>
- Artificial intelligence based control <sup>[11],[12]</sup>, etc...

Stimulated by the idea of linear internal model control <sup>[13]</sup>, we developed a nonlinear internal model controller for an induction motor <sup>[17]</sup>. Simulation results in [17] show that the proposed controller has good performance and robustness against variations in motor parameters. This paper continues the work in [17] and reports results on a real system. The proposed controller has been used to control two squirrel induction motors, the power of which are 0.5HP and 3HP. Experimental results show that the proposed controller is effective and robust against variation in motor parameters.

The remainder of the paper is as follows: Section 2 recalls the model of an induction motor. Section 3 describes the proposed control system. Section 4 presents the simulation results. Section 5 gives results on real systems while Section 6 concludes the paper.

Manuscript received January 15, 2009; revised April 03, 2009

<sup>†</sup>Corresponding Author: dhnghia@hcmut.edu.vn

Tel: +84.838647256, Fax: +84.838647256, Univ. of Technology  
<sup>\*</sup>Dept. of Electrical and Electronics Eng., Hochiminh City Univ.  
of Technology, Vietnam.

<sup>\*\*</sup>School of Electrical Engineering, University of Ulsan, Korea

## 2. Model of Induction Motor

The state space model of an induction motor in the DQ co-ordinate is given by (1)-(6) [3],[15],

$$\frac{di_{sd}}{dt} = -a_1 i_{sd} + \omega_s i_{sq} + a_2 \Psi_{rd} + a_3 \omega \Psi_{rq} + a_4 u_{sd} \quad (1)$$

$$\frac{di_{sq}}{dt} = -\omega_s i_{sd} - a_1 i_{sq} - a_3 \omega \Psi_{rd} + a_2 \Psi_{rq} + a_4 u_{sq} \quad (2)$$

$$\frac{d\Psi_{rd}}{dt} = a_5 i_{sd} - a_5 \Psi_{rd} + (\omega_s - \omega) \Psi_{rq} \quad (3)$$

$$\frac{d\Psi_{rq}}{dt} = a_5 i_{sq} - (\omega_s - \omega) \Psi_{rd} - a_5 \Psi_{rq} \quad (4)$$

$$T_e = a_6 [\Psi_{rd} i_{sq} - \Psi_{rq} i_{sd}] \quad (5)$$

$$\frac{d\omega}{dt} = a_7 [T_e - T_L] \quad (6)$$

where  $(i_{sd}, i_{sq})$ ,  $(u_{sd}, u_{sq})$ ,  $(\Psi_{rd}, \Psi_{rq})$  are, respectively, the stator current (A), the stator voltage (V), and the normalized rotor flux (A) the DQ co-ordinate,  $\omega$  is the rotor speed (rad/s),  $T_e$  is the motor torque (Nm),  $T_L$  is the load torque (Nm),  $\omega_s$  is the synchronous speed of a p-pole motor (rad/s),

$$a_1 = \left( \frac{1}{\sigma T_s} + \frac{1-\sigma}{\sigma T_r} \right), \quad a_2 = \frac{1-\sigma}{\sigma T_r}, \quad a_3 = \frac{1-\sigma}{\sigma} \quad (7)$$

$$a_4 = \frac{1}{\sigma L_s}, \quad a_5 = \frac{1}{T_r}, \quad a_6 = \frac{3pL_m^2}{2L_r}, \quad a_7 = \frac{p}{J} \quad (8)$$

$$\sigma = 1 - \frac{L_m^2}{L_s L_r}, \quad T_s = \frac{L_s}{R_s}, \quad T_r = \frac{L_r}{R_r} \quad (9)$$

are constants,  $R_s$  is the stator resistance,  $R_r$  is the rotor resistance,  $L_s$  is the stator inductance,  $L_r$  is the rotor inductance,  $L_m$  is the mutual inductance,  $p$  is the number of pole pairs, and  $J$  is the moment of inertia of the rotor.

Define

$$\Psi_r = \sqrt{\Psi_{rd}^2 + \Psi_{rq}^2} \quad (10)$$

The control objective is to regulate the rotor flux  $\Psi_r$  and the rotor speed  $\omega$  at the set point values,  $r_\psi$  and  $r_\omega$  respectively.

## 3. The Control System

### 3.1 The internal model controller

The control system is depicted in Fig. 1 where the process model is a model of the inverter and the induction motor. It has inputs  $u_{sd}$ ,  $u_{sq}$ ,  $\omega_s$  and outputs  $\bar{\Psi}_r$ ,  $\bar{\omega}$ . If the process model is exact and if there is no disturbance ( $T_L \equiv 0$ ), then the outputs of the process model must be equal to the outputs of the induction motor

$$\bar{\Psi}_r = \Psi_r \quad \text{and} \quad \bar{\omega} = \omega \quad (11)$$

The inverse model is an inverse of the process model. It has inputs  $\tilde{\Psi}_r$ ,  $\tilde{\omega}$  and outputs  $u_{sd}$ ,  $u_{sq}$ ,  $\omega_s$ . If the inverse model is exact then the inputs of the inverse model must be equal to the outputs of the process model

$$\tilde{\Psi}_r = \bar{\Psi}_r \quad \text{and} \quad \tilde{\omega} = \bar{\omega} \quad (12)$$

If the process model and the inverse model are exact and if there is no disturbance then it follows from (11) and (12) that

$$\tilde{\Psi}_r = \Psi_r \quad \text{and} \quad \tilde{\omega} = \omega \quad (13)$$

Moreover, (11) implies that the feedback signals are null, it follows that

$$r_\psi = e_\psi \quad \text{and} \quad r_\omega = e_\omega \quad (14)$$

Where  $r_\psi$  and  $r_\omega$  are the desired output of  $\Psi_r$  and  $\omega$ , respectively,

$$e_\psi = r_\psi - (\psi_r - \bar{\psi}_r)$$

and 
$$e_\omega = r_\omega - (\omega - \bar{\omega})$$

From Fig. 1, it can be seen that the transfer functions from the set point signals  $r_\psi$  and  $r_\omega$  to the output signals  $\Psi_r$  and  $\omega$  are the exact transfer functions of the IMC filters. We can thus assign the transfer function of the closed loop system by choosing an appropriate IMC filter.

### 3.2 The process model

The process model is derived from (1)-(6) with  $T_L = 0$  ( $T_L$  is considered as disturbance)

$$\frac{d\bar{i}_{sd}}{dt} = -\hat{a}_1 \bar{i}_{sd} + \omega_s \bar{i}_{sq} + \hat{a}_2 \bar{\Psi}_{rd} + \hat{a}_3 \bar{\omega} \bar{\Psi}_{rq} + \hat{a}_4 u_{sd} \quad (15)$$

$$\frac{d\bar{i}_{sq}}{dt} = -\omega_s \bar{i}_{sd} - \hat{a}_1 \bar{i}_{sq} - \hat{a}_3 \bar{\omega} \bar{\Psi}_{rd} + \hat{a}_2 \bar{\Psi}_{rq} + \hat{a}_4 u_{sq} \quad (16)$$

$$\frac{d\bar{\Psi}_{rd}}{dt} = \hat{a}_5 \bar{i}_{sd} - \hat{a}_5 \bar{\Psi}_{rd} + (\omega_s - \bar{\omega}) \bar{\Psi}_{rq} \quad (17)$$

$$\frac{d\bar{\Psi}_{rq}}{dt} = \hat{a}_5 \bar{i}_{sq} - (\omega_s - \bar{\omega}) \bar{\Psi}_{rd} - \hat{a}_5 \bar{\Psi}_{rq} \quad (18)$$

$$\bar{T}_e = \hat{a}_6 [\bar{\Psi}_{rd} \bar{i}_{sq} - \bar{\Psi}_{rq} \bar{i}_{sd}] \quad (19)$$

$$\frac{d\bar{\omega}}{dt} = \hat{a}_7 \bar{T}_e \quad (20)$$

$$\bar{\Psi}_r = \sqrt{\bar{\Psi}_{rd}^2 + \bar{\Psi}_{rq}^2} \quad (21)$$

where  $\hat{a}_1 - \hat{a}_7$  are defined similarly to  $a_1 - a_7$  in (7)-(9) with the estimated values of the parameters of the motor.

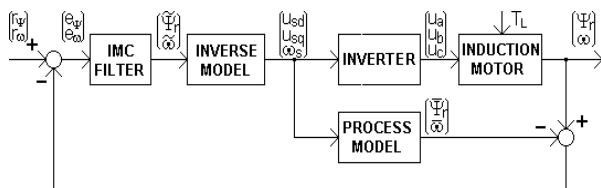


Fig. 1. The internal model control system.

### 3.3 The inverse model

The inverse model is developed from (1)-(6) as follows

$$\frac{d\tilde{i}_{sd}}{dt} = -\hat{a}_1 \tilde{i}_{sd} + \omega_s \tilde{i}_{sq} + \hat{a}_2 \tilde{\Psi}_{rd} + \hat{a}_3 \tilde{\omega} \tilde{\Psi}_{rq} + \hat{a}_4 u_{sd} \quad (22)$$

$$\frac{d\tilde{i}_{sq}}{dt} = -\omega_s \tilde{i}_{sd} - \hat{a}_1 \tilde{i}_{sq} - \hat{a}_3 \tilde{\omega} \tilde{\Psi}_{rd} + \hat{a}_2 \tilde{\Psi}_{rq} + \hat{a}_4 u_{sq} \quad (23)$$

$$\frac{d\tilde{\Psi}_{rd}}{dt} = \hat{a}_5 \tilde{i}_{sd} - \hat{a}_5 \tilde{\Psi}_{rd} + (\omega_s - \tilde{\omega}) \tilde{\Psi}_{rq} \quad (24)$$

$$\frac{d\tilde{\Psi}_{rq}}{dt} = \hat{a}_5 \tilde{i}_{sq} - (\omega_s - \tilde{\omega}) \tilde{\Psi}_{rd} - \hat{a}_5 \tilde{\Psi}_{rq} \quad (25)$$

$$\tilde{T}_e = \hat{a}_6 [\tilde{\Psi}_{rd} \tilde{i}_{sq} - \tilde{\Psi}_{rq} \tilde{i}_{sd}] \quad (26)$$

$$\frac{d\tilde{\omega}}{dt} = \hat{a}_7 \tilde{T}_e \quad (27)$$

$$\tilde{\Psi}_r = \sqrt{\tilde{\Psi}_{rd}^2 + \tilde{\Psi}_{rq}^2} \quad (28)$$

where  $\hat{a}_1 - \hat{a}_7$  are the same parameters as in (15)-(21). Without loss of generality we can suppose that  $\tilde{\Psi}_{rq} = 0$  then  $\tilde{\Psi}_{rd} = \tilde{\Psi}_r$ . This, together with (26) and (27), yields

$$\tilde{i}_{sq} = \frac{1}{\hat{a}_6 \hat{a}_7 \tilde{\Psi}_r} \frac{s \tilde{\omega}}{T_d s + 1} \quad (29)$$

where  $s$  is the Laplace operator,  $T_d$  is a time constant, the transfer function  $s/(T_d s + 1)$  is used to approximate the derivative operator  $d/dt$ . Similarly, it follows from (24) that

$$\tilde{i}_{sd} = \hat{T}_r \frac{s \tilde{\Psi}_r}{T_d s + 1} + \tilde{\Psi}_r \quad (30)$$

where  $\hat{T}_r = \frac{1}{\hat{a}_5}$ . Since  $\tilde{\Psi}_{rq} = 0$ , (25) yields

$$\omega_s = \tilde{\omega} + \frac{\tilde{i}_{sq}}{T_r \tilde{\Psi}_r} \quad (31)$$

Finally (22) and (23) become

$$u_{sd} = \frac{1}{\hat{a}_4} \left[ \frac{s \tilde{i}_{sd}}{T_d s + 1} + \hat{a}_1 \tilde{i}_{sd} - \omega_s \tilde{i}_{sq} - \hat{a}_2 \tilde{\Psi}_r \right] \quad (32)$$

$$u_{sq} = \frac{1}{\hat{a}_4} \left[ \frac{s \tilde{i}_{sq}}{T_d s + 1} + \omega_s \tilde{i}_{sd} + \hat{a}_1 \tilde{i}_{sq} + \hat{a}_3 \tilde{\omega} \tilde{\Psi}_r \right] \quad (33)$$

The inverse model is defined by (26)-(33).

### 3.4 The IMC filter

The IMC filters are low pass filters

$$F_\omega(s) = \frac{1}{\tau_\omega s + 1} \quad (34)$$

and 
$$F_\Psi(s) = \frac{1}{\tau_\Psi s + 1} \quad (35)$$

where  $\tau_\omega$  and  $\tau_\Psi$  are time constants which determine the response time of the closed loop system. Note that the static gain of both filters is 1.

### 3.5 The rotor flux observer

In practice the rotor flux is rarely available. We often have to estimate the rotor flux to use in the control system as shown in Fig. 2. The rotor flux estimator has inputs  $u_{sd}$ ,  $u_{sq}$ ,  $\omega_s$ ,  $i_{sd}$ ,  $i_{sq}$ , and output  $\hat{\Psi}_r$ , an estimated value for  $\Psi_r$ . The estimator can be derived from (1)-(4) as follows

$$\frac{d\hat{i}_{sd}}{dt} = -\hat{a}_1 \hat{i}_{sd} + \hat{\omega}_s \hat{i}_{sq} + \hat{a}_2 \hat{\Psi}_{rd} + \hat{a}_3 \omega \hat{\Psi}_{rq} + \hat{a}_4 u_{sd} - K_0 [i_{sd} - \hat{i}_{sd}] \quad (36)$$

$$\frac{d\hat{i}_{sq}}{dt} = -\hat{\omega}_s \hat{i}_{sd} - \hat{a}_1 \hat{i}_{sq} - \hat{a}_3 \omega \hat{\Psi}_{rd} + \hat{a}_2 \hat{\Psi}_{rq} + \hat{a}_4 u_{sq} - K_0 [i_{sq} - \hat{i}_{sq}] \quad (37)$$

$$\frac{d\hat{\Psi}_{rd}}{dt} = \hat{a}_5 i_{sd} - \hat{a}_5 \hat{\Psi}_{rd} + (\hat{\omega}_s - \omega) \hat{\Psi}_{rq} - K_0 [i_{sd} - \hat{i}_{sd}] \quad (38)$$

$$\frac{d\hat{\Psi}_{rq}}{dt} = \hat{a}_5 i_{sq} - (\hat{\omega}_s - \omega) \hat{\Psi}_{rd} - \hat{a}_5 \hat{\Psi}_{rq} - K_0 [i_{sq} - \hat{i}_{sq}] \quad (39)$$

$$\hat{\Psi}_r = \sqrt{\hat{\Psi}_{rd}^2 + \hat{\Psi}_{rq}^2} \quad (40)$$

where  $\hat{a}_1 - \hat{a}_7$  are the same parameters as in (15)-(21). Note that the terms

$$K_0 (i_{sd} - \hat{i}_{sd}) \quad \text{and} \quad K_0 (i_{sq} - \hat{i}_{sq})$$

in (36) and (37) are the correction terms of the state observer [16].

Table 1 The parameters of the motor

$R_s$ ( $\Omega$ )	$R_r$ ( $\Omega$ )	$L_s$ (H)	$L_r$ (H)	$L_m$ (H)	$p$	$J$ ( $\text{Kgm}^2$ )
1.177	1.382	0.119	0.118	0.113	2	0.00126

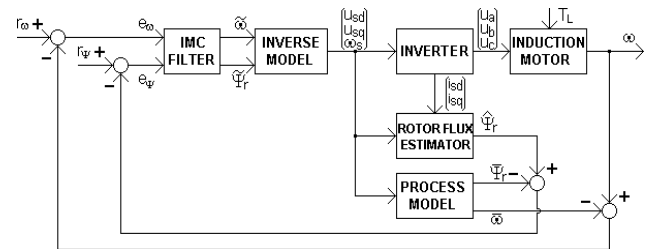


Fig. 2. The IMC system with rotor flux estimator.

## 4. Simulation Results

The parameters of the motor are given in table 1. The parameters of the process model and the inverse model are the same as the motor. The parameters of the controller are chosen as follows: the time constant of the IMC filters  $\tau_\omega = 0.3s$  and  $\tau_\Psi = 0.05s$  (which correspond to the response times  $3\tau_\omega = 0.9s$  and  $3\tau_\Psi = 0.15s$ , respectively). Since  $i_{sd}$ ,  $i_{sq}$ ,  $\omega$ , and  $\Psi_r$  vary slowly, we choose  $T_d = 1ms$ . The rotor flux estimator is designed with  $K_0 = 10$ . In the simulation, the motor is accelerated at  $t = 0s$  to  $150\text{rad/s}$  without load. The load  $T_L = 3.5\text{Nm}$  is introduced at  $t = 1.5s$ . At  $t = 2s$  the motor is decelerated to  $75\text{rad/s}$ .

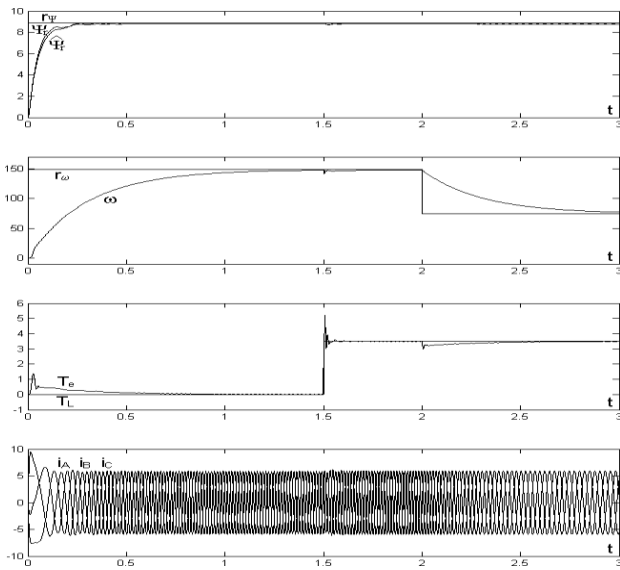


Fig. 3. Response of the control system to step input.

Fig. 3 shows the response of the control system. Observe that

- The response time of the rotor flux  $\Psi_r$  is about  $3\tau_\Psi = 0.15s$ .
- The response time of the rotor speed  $\omega$  is about  $3\tau_\omega = 0.9s$ .
- The static errors of the rotor flux and rotor speed are null.

This simulation shows that we can easily specify the desired performance of the control system via the IMC filters. More simulation results are given in [17] which shows that the proposed control system is robust against variation in motor parameters and that the IMC filter can be used to tune the robustness of the controller.

### 5. Experiment Results

The hardware set up (Fig.4) is composed of:

- a dSpace DS1104 kit.
- a three level inverter (Fig.5) with 12 IGBTs (FGL60N100BNTD) and 2 capacitors (4700uF/200V).
- the stator current sensors are 2 LA25A-NP LEM.
- the rotor speed sensor is an encoder (with 2048 pulse resolution).
- the load is a DC generator.

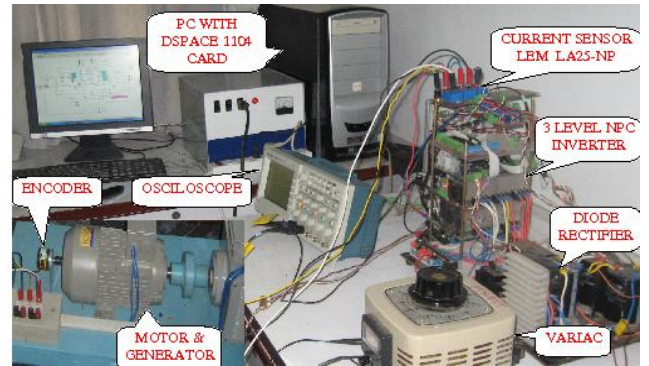


Fig. 4. Experimental setup.

In order to test the robustness of the controller, the experimental results were carried out with two different motors (with power 3 HP and 0.5 HP). The parameters of these motors are given in table 2.

Table 2 The parameters of two motors

Parameters	3HP Motor	0.5HP Motor
$R_s (\Omega)$	1.97	13
$R_r (\Omega)$	1.96	13
$L_s (H)$	0.37	0.04
$L_r (H)$	0.37	0.04
$L_m (H)$	0.36	0.03
$p$	1	2
$J (Kg\cdot m^2)$	0.002	0.0007
Rate voltage (V)	230/400	220/380
Rate current (A)	7.9/4.55	2.1/1.2
Rate rotor speed (rad/s)	300	148

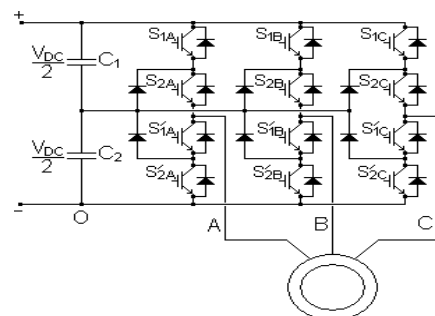


Fig. 5. The three-level inverter.

Both motors are controlled by the same IMC controller which is designed in section IV and with model parameters given in table 1 (with the 3 HP motor, a value of  $p = 1$  has been used for the process model and the inverse model). The results are given in Fig. 6-10 (for 3HP motor) and in Fig. 11-14 (for 0.5HP motor). Remark that

- The response of the control system is governed by the IMC filters in a large range of motor parameters (the response time of the rotor speed is around  $3\tau_{\omega} = 0.9s$  in all cases).
- The rotor speed and the rotor flux are almost not sensible to the change of the load.

### 6. Conclusion

Based on the nonlinear IMC approach this paper describes a novel method for induction motor control. Both process model and inverse model are nonlinear and are given in the rotor flux coordinate. The main advantage of the proposed method follow from the fact that the transfer functions of the closed loop system is exactly the same as the IMC filters. The desired performance (the steady state error, the response time, the transient response, etc.) of the control system can be easily specified and effective via the IMC filters.

Simulation results illustrate the effectiveness of the proposed method. Results on a real time system reveal that the proposed controller has good performance and is not sensible to changes in motor parameters.

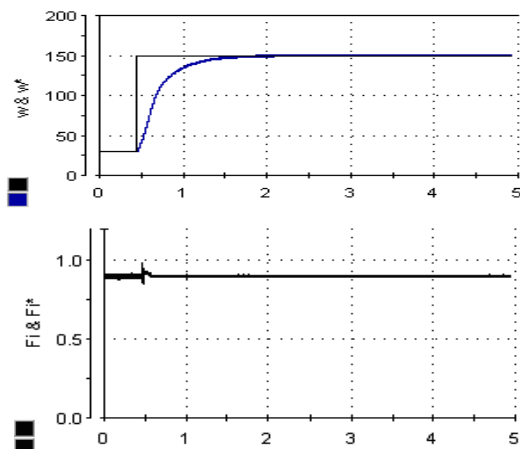


Fig. 6. No load acceleration (3HP motor): Rotor speed (upper) and rotor flux (lower).

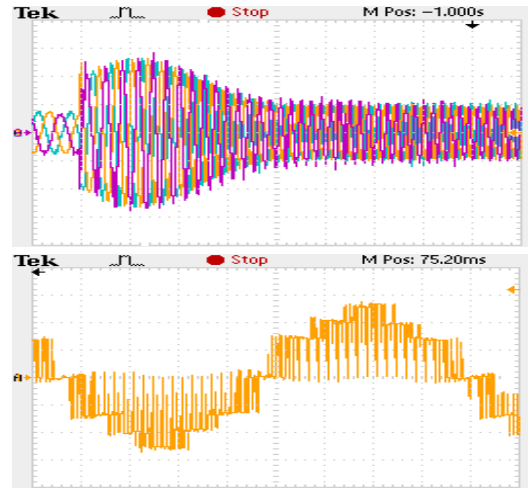


Fig. 7. No load acceleration (3HP motor): Stator current (upper) and stator voltage (lower).

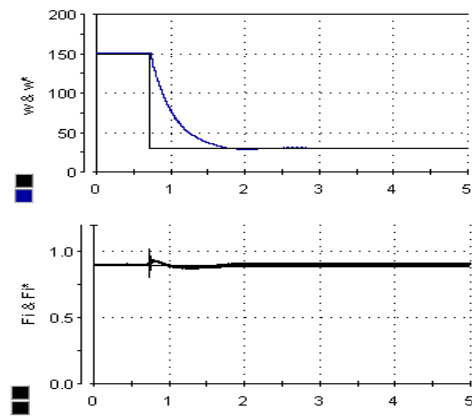


Fig. 8. No load deceleration (3HP motor): Rotor speed (upper) and rotor flux (lower).

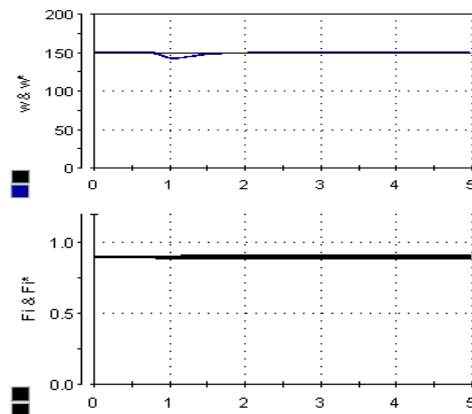


Fig. 9. Speed response to step change in torque demand from 0 to 1.5 Nm (3HP motor): Rotor speed (upper) and rotor flux (lower).

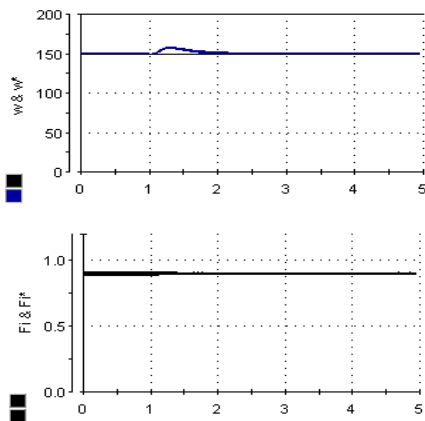


Fig. 10. Response to cancellation of load (1.5Nm, 3HP motor): Rotor speed (upper) and rotor flux (lower).

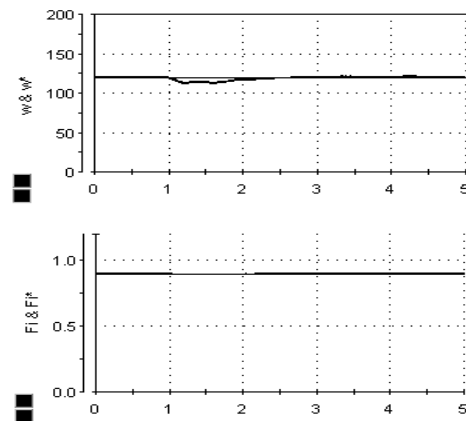


Fig. 13. Speed response to step change in torque demand from 0 to 1.5 Nm (0.5HP motor): Rotor speed (upper) and rotor flux (lower).

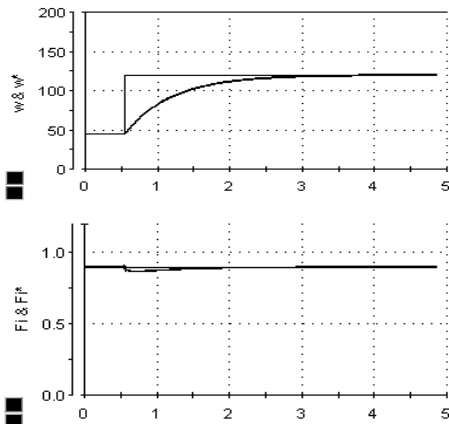


Fig. 11. No load acceleration (0.5HP motor): Rotor speed (upper) and rotor flux (lower).

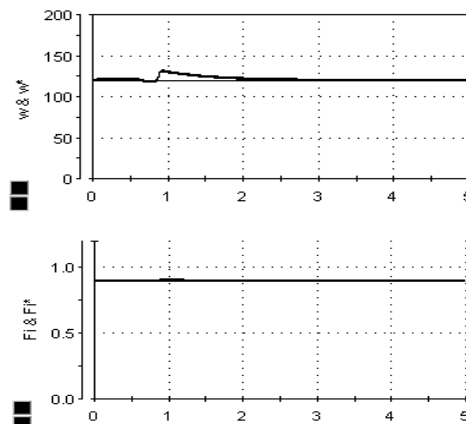


Fig. 14. Response to cancellation of load (1.5Nm, 0.5HP motor): Rotor speed (upper) and rotor flux (lower).

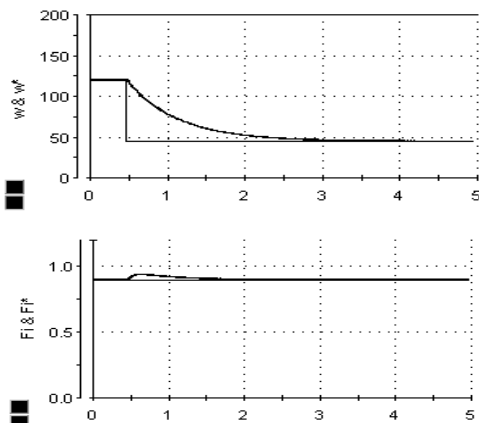


Fig. 12. No load deceleration (0.5HP motor): Rotor speed (upper) and rotor flux (lower).

### References

- [1] A. S. Elwer, "A Novel Technique for Tuning PI-Controllers in Induction Motor Drive Systems for Electric Vehicle Applications," *Journal of Power Electronics*, Vol. 6, No. 4, pp.322-329, 2006.
- [2] A.M. Trzynadlowski, *The Orientation Principle in Control of Induction Motors*, Kluwer Academic Publishers, 1994.
- [3] C. Canudas de Wit (ed.), *Modelisation, controle vectoriel et DTC*, Hermes Science, 2000.
- [4] C. Lascu, I Boldea, F. Blaabjerg. "A modified direct torque control for induction motor sensorless drive," *IEEE Transaction on Industrial Application*, Vol.36, Issue 1, pp.122-130, Jan/Feb 2000.
- [5] H.H.Lee, M.Ng. Hoang, T.W. Chun, "Implementation of

Direct Torque Control Method using Matrix Converter Fed Induction Motor,” *Journal of Power Electronics*, Vol.8, No.1, pp.74-80, 2008.

- [6] R. Ortega, A. Loria, P.J. Nicklasson and H. Sira-Ramírez, Passivity-Based Control Of Euler-Lagrange System. Mechanical, Electrical And Electromechanical Applications, Springer, 1998.
- [7] C. Cecati, N. Rotondal, “Torque and Speed Regulation of Induction Motor Using the Passivity Theory Approach,” *IEEE Transaction on Industrial Electronics*, Vol. 46, No. 1, pp.119-126, April 1999.
- [8] E.H.E.Bayoumi, M.N.F. Nashed, “A Fuzzy Predictive Sliding Mode Control for High Performance Induction Motor Position Drives,” *Journal of Power Electronics*, Vol. 5, No.1, pp.20-28, 2005.
- [9] V.I. Utkin, J. Guldner, J. Shi, Sliding mode control in electromechanical systems, Taylor & Francis, 1999.
- [10] A. Benchaid, A. Rachid, E. Audrezet, “Sliding Mode Input-Output Linearization and Field Orientation for Real-Time Control of Induction Motors,” *IEEE Transactions on Power Electronics*, Vol.14, No.1, pp.3-13. 1999.
- [11] P. Vas, Artificial-Intelligence-Based Electrical Machines And Drives. Application of Fuzzy, Neural, Fuzzy-Neural, and Genetic-Algorithm-Based Techniques, Oxford University Press, 1998.
- [12] M.M. Salem, “Classical Controller with Intelligent Properties for Speed Control of Vector Controlled Induction Motor,” *Journal of Power Electronics*, Vol.8, No.3, pp.210-216, 2008.
- [13] M. Morari, E. Zafiriou, Robust process control, Prentice Hall, 1997.
- [14] R. Berber, Methods of model based process control, Kluwer Academic Publishers, 1994.
- [15] W. Leonhard, Control of electrical drives, Springer, Verlag, 1985.
- [16] H.K. Khalil, Nonlinear systems, Prentice-Hall, 2002.
- [17] Duong Hoai Nghia, Nguyen Van Nho, Hong-Hee Lee, Control of induction motor using IMC approach, ICPE’07 Conference in Daegu, Korea, 2007.



**Duong Hoai Nghia** was born in Vietnam, in 1957. He received his M.S. and PhD. degrees in Electrical Engineering from the Institut National Polytechnique de Grenoble, France in 1989 and 1993, respectively. Since 1981, he has been with the Department of Electrical and Electronics Engineering, Ho Chi Minh City University of

Technology, Vietnam, where he is currently an associate professor. His research interests are in the areas of control engineering.



**Nguyen Van Nho** was born in Vietnam, in 1964. He received his M.S. and PhD. degrees in Electrical Engineering from the University of West Bohemia, Czech Republic in 1988 and 1991, respectively. Since 1992, he has been with Department of Electrical and Electronics Engineering, Ho Chi Minh City University of Technology, Vietnam, where he is currently Associate Professor. He has been with KAIST as a post-doc fellow for six months in 2001 and as a visiting professor for a year in 2003-2004. His research interests are in the areas of modeling and control of ac motors, active filters and PWM techniques.



**Nguyen Xuan Bac** was born in Vietnam, in 1984. He received his B.S. degree in Automatic Control Engineering from the University of Technology, Ho Chi Minh, Vietnam in 2007 and is currently a M.S. student at the University of Technology, Vietnam. He is also a lecturer of Electrical and Electronics Engineering Department, Ho Chi Minh City University of Technology. His research interests are in advanced control of electrical machines and power electronics.



**Hong-Hee Lee** received his B.S., M.S., and Ph.D. degrees from Seoul National University, Seoul, Korea. Currently, he is a Professor at the School of Electric-Electronic Information System Engineering, University of Ulsan, Korea. He is also the Director of the Network-based Automation Research Center (NARC), which is sponsored by the Ministry of Commerce, Industry and Energy (MOCIE). His research interests are power electronics, network-based motor control, and control network. He is a member of IEEE, KIEE, KIPE, and ICROS.